

# Magnesian-riebeckite from the Varenche mine (Aosta Valley, Italy): crystal-chemical characterization of a grandfathered end-member

ROBERTA OBERTI<sup>1,\*</sup>, MASSIMO BOIOCCHI<sup>2</sup>, FRANK C. HAWTHORNE<sup>3</sup> AND MARCO E. CIRIOTTI<sup>4</sup>

<sup>1</sup> CNR-Istituto di Geoscienze e Georisorse, Sede secondaria di Pavia, via Ferrata 1, I-27100 Pavia, Italy

<sup>2</sup> Centro Grandi Strumenti, Università di Pavia, via Bassi 21, I-27100 Pavia, Italy

<sup>3</sup> Department of Geological Sciences, University of Manitoba, Winnipeg, Manitoba, R3T 2N2, Canada

<sup>4</sup> Associazione Micromineralogica Italiana, via San Pietro 55, I-10073 Devesi-Cirié, Italy

[Received 2 January 2017; Accepted 6 February 2017; Associate Editor: Giancarlo Della Ventura]

## ABSTRACT

Magnesian-riebeckite from the dumps of the abandoned mine of Varenche (45°47'22" N, 7°29'17" E), Saint-Barthélemy, Nus, Aosta Valley (Italy), was studied to provide the complete mineral description (including crystal structure) and insights into the crystal-chemistry of riebeckite. The empirical formula derived from electron microprobe analysis and single-crystal structure refinement is  ${}^A(\text{Na}_{0.09}\text{K}_{0.01})_{\Sigma=0.10} {}^B(\text{Na}_{1.77}\text{Ca}_{0.11}\text{Mg}_{0.08}\text{Mn}_{0.04}^{2+})_{\Sigma=2.00} {}^C(\text{Mg}_{2.93}\text{Mn}_{0.13}\text{Fe}_{0.07}^{2+}\text{Zn}_{0.01}\text{Ni}_{0.12}\text{Fe}_{1.25}^{3+}\text{Al}_{0.48}\text{Ti}_{0.01})_{\Sigma=5.00} {}^T(\text{Si}_{7.92}\text{Al}_{0.08})_{\Sigma=8.00} \text{O}_{22} {}^W(\text{OH}_{1.88}\text{F}_{0.12})_{\Sigma=2.00}$ . Magnesian-riebeckite is biaxial (+), with  $\alpha = 1.678(2)$ ,  $\beta = 1.682(2)$ ,  $\gamma = 1.688(2)$  and  $2V$  (meas.) = 80.2(1.7)°,  $2V$  (calc.) = 78.7°. The unit-cell parameters are  $a = 9.6481(14)$ ,  $b = 17.873(3)$ ,  $c = 5.3013(7)$  Å,  $\beta = 103.630(2)^\circ$ ,  $V = 888.4(2)$  Å<sup>3</sup>,  $Z = 2$ , space group  $C2/m$ . The strongest ten reflections in the powder X-ray pattern [ $d$  values (in Å),  $I$ , ( $hkl$ )] are: 2.701, 100, (151); 8.303, 83, (110); 3.079, 62, (310); 3.391, 53, (131); 4.467, 50, (040,021); 2.522, 50, ( $\bar{2}02$ ); 2.578, 35, (061); 2.155, 30, (261), 4.855, 30, ( $\bar{1}11$ ), 2.300, 29, ( $\bar{3}51$ ).

**KEYWORDS:** magnesian-riebeckite, electron microprobe analysis, optical properties, powder-diffraction pattern, crystal-structure refinement, Varenche mine, Italy.

## Introduction

THE name 'riebeckite' was first used by Sauer (1888) when describing a blackish amphibole collected in Socotra (Yemen) by Dr. E. Riebeck. The first refinements of the crystal structures of magnesian-riebeckite and riebeckite were done by Whittaker (1949) and Colville and Gibbs (1964), respectively. However, complete physical, chemical and crystallographic data on a single sample are missing in the literature. A complete characterization of the RT and HT behaviour of riebeckite from Malawi with composition close to the ideal end-member  ${}^B\text{Na}_2{}^C(\text{Fe}_3^{3+}\text{Fe}_2^{3+}){}^T\text{Si}_8\text{O}_{22}{}^W(\text{OH})_2$ , has

been recently reported in Susta (2016) using electron microprobe analysis (EMPA) and laser ablation inductively coupled plasma mass spectrometry, single-crystal and powder X-ray diffraction, and Mössbauer FTIR and Raman spectroscopy (at RT and HT); and Hawthorne (1978) reported a refinement of the crystal structure of fluororriebeckite. Susta (2016; more detail in Oberti *et al.*, 2018) reported some unique peculiarities in riebeckite at high temperature, such as migration of B cations to the A site after complete deprotonation. A better understanding of this behaviour requires investigation of a Mg-rich composition, and this fact prompted the search for well-characterized samples of magnesian-riebeckite, ideally  ${}^B\text{Na}_2{}^C(\text{Mg}_3\text{Fe}_2^{3+}){}^T\text{Si}_8\text{O}_{22}{}^W(\text{OH})_2$ . While doing this, we realized that a complete characterization of magnesian-riebeckite was missing in the literature.

\*E-mail: oberti@crystal.unipv.it

<https://doi.org/10.1180/minmag.2017.081.011>

The name magnesio-riebeckite was first used by Myiashiro and Iwasaki (1957) when reporting on a strongly zoned crystal collected at Bizan, a hill in the city of Tokushima (Sanbagawa-Mikabu zone, Shikoku), which is one of the most famous localities for glaucophane and piemontite in Japan. The alkali-deficient host-rock is a garnet-aegirine-amphibole-muscovite-quartz-schist with some hematite and 'apatite'. Magnesio-riebeckite may have formed during recrystallization under the conditions of glaucophanitic metamorphism, not necessarily because of alkali metasomatism. Myiashiro (1957) noted that riebeckite and magnesio-riebeckite have a large excess of alkalis over the alkali/alumina ratio of alkali feldspar, and concluded that their crystallization is related to excess alkalis in the rocks. This condition is fulfilled in: (a) alkalic igneous rocks (Sørensen, 1974; Le Bas *et al.*, 1986) and their metamorphic derivatives; (b) rocks in which the composition was significantly modified by alkali metasomatism. Therefore, the occurrence of riebeckite and magnesio-riebeckite is limited. Riebeckite and magnesio-riebeckite were synthesized by Ernst (1957–1959, 1962), who found that the upper stability limit of riebeckite is 400°C lower than that of magnesio-riebeckite; the substitution of F for OH also increases the thermal stability of the mineral, and F-rich riebeckite may occur at magmatic conditions (Ernst, 1968). Myiashiro and Iwasaki (1957) provided a chemical analysis and the optical properties of magnesio-riebeckite, but did not report on the crystal structure and crystal chemistry. Bonazzi *et al.* (1996) and Barresi *et al.* (2005) cited a potential magnesio-riebeckite at the Varenche mine; hence we focused our search on that locality.



FIG. 1. The rock specimen studied in this work (UK10), containing bladed pale-yellow crystals of magnesio-riebeckite in a dark-grey matrix associated with quartz.

*et al.* (1979), the circulating seawater leached Si, Cu, Fe, Mn and other metals from the basaltic rocks, and was also enriched in S, Cu and Fe that precipitated as sulfides around submarine hydrothermal vents, while quartz and braunite are common in the surrounding rocks. All mineralization recrystallized and was deformed during the Alpine orogeny (Castello, 1981).

In the Varenche area, the mineralization occurs in the lower part of a band of quartz schist, up to 20 m thick (Fig. 3) that contains 'fuchsite'; this horizon is part of a series of metamorphosed sediments (schist, chloritoschist, quartzites, schists *s.s.*) associated with large bodies of serpentinite. The quartzites of Varenche (Baldelli *et al.*, 1983) are dominantly greenschist facies of probable

### Occurrence and optical properties

The specimen studied in this work (UK10, Fig. 1) was found by M.E.C. in the dumps of the abandoned mine of Varenche (45°47'22" N, 7°29'17" E), Saint-Barthélemy, Nus, Aosta Valley (Italy).

The area close to the abandoned Varenche mine shows typical mineralization associated with Mn in quartzitic rocks in the Piedmont greenschist complex ('Pietre Verdi') in the Western Alps (Fig. 2). These deposits are often associated with concentrations of iron and copper sulfides, and were formed in a marine environment, associated with an exhalative hydrothermal vent associated with ophiolitic volcanism. According to Dal Piaz



FIG. 2. Quartz schists in the dump of the abandoned Varenche mine.

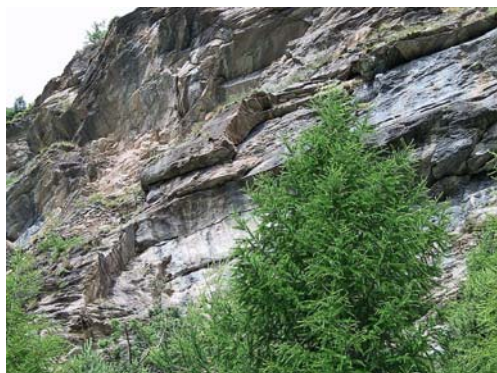


FIG. 3. The quartz schist (~20 m thick) in the Varenche field.

mesoalpine age, and relics of an earlier high-*P* metamorphic stage consisting of Na amphibole, Mn-rich chloritoid and almandine. Both stratigraphy and mineralization are consistent with hydrothermal activity in fracture zones; there is no genetic correlation between Mn and Cr in the fuchsite micas.

Many mineral species occur at the Varenche abandoned mine: aegirine, albite, almandine, aragonite, ardennite-(As), ardennite-(V), arsenio-pleite, azurite, baryte, birnessite, braunite, brochantite, calcite, chalcopyrite, chloritoid, chrysotile, clinocllore, clinohumite, covellite, danburite, djurleite, dolomite, epidote, grossular, hematite, hydroxyapatite, jadeite, kutnohorite, magnetite, malachite, manganberzeliite, muscovite, orthoclase, phlogopite, piemontite, pyrite, pyrolusite, pyrophanite, quartz, ranciéite, rhodochrosite, rutile, saponite, sarkinite, siderite, spessartine, sphalerite, sursassite, talc, tephroite, thortveitite, todorokite, vesuvianite, a new arsenate Sc-dominant analogue of metavariscite and a series of other amphiboles not yet characterized. Magnesio-riebeckite occurs as sub-millimetre bladed pale-yellow crystals embedded in a dark-grey matrix and associated with quartz.

A spindle stage was used to orient a crystal for measurement of refractive indices and 2*V* by extinction curves (Bartelmehs *et al.*, 1992). The optical orientation was determined by transferring the crystal from the spindle stage to a single-crystal diffractometer and measuring the relative axial relations by X-ray diffraction. In transmitted plane-polarized light, magnesio-riebeckite is slightly pleochroic (*X* = very pale yellow, *Y* = pale yellow, *Z* = pale yellow-brown), non-fluorescent, and has a

vitreous lustre. It is biaxial (+),  $\alpha = 1.678(2)$ ,  $\beta = 1.682(2)$ ,  $\gamma = 1.688(2)$ , 2*V* (meas) = 80.2(1.7), 2*V* (calc) = 78.7°. The dispersion is weak ( $v > r$ ), and the orientation is:  $X \wedge c = 9^\circ$  (in  $\beta$  obtuse),  $Y \parallel b$ ,  $Z \wedge c = 5^\circ$  (in  $\beta$  obtuse). The compatibility index ( $1 - (K_p/K_c)$ ) is 0.008 (superior).

### Single-crystal diffraction and powder analysis

Diffraction data for a lamellar single crystal  $130 \mu\text{m} \times 100 \mu\text{m} \times 60 \mu\text{m}$  in size (1303 in the amphibole database at CNR-IGG Pavia) were collected in the  $\theta$  range 2–30° with a Bruker-AXS CCD diffractometer, with graphite-monochromatized MoK $\alpha$  X-radiation ( $\lambda = 0.7107 \text{ \AA}$ ). Omega rotation frames (scan width = 0.4°, scan time = 30 s, sample-to-detector distance = 50 mm) were processed with the *SAINTE* software (Bruker, 2003) and intensities were corrected for Lorentz and polarization effects; absorption effects were empirically evaluated with the *SADABS* software (Krause *et al.*, 2015) and an absorption correction was applied to the data. A total of 8207 collected reflections was reduced to 1355 unique reflections (mean redundancy = 6,  $R_{\text{int}} = 1.6\%$ ). Of these, 1207 reflections with  $I_o > 3 \sigma I$  were considered as observed during unweighted full-matrix least-squares refinement on *F*. Scattering curves for fully ionized chemical species were used at sites where chemical substitutions occur; neutral vs. ionized scattering curves were used at the *T* and anion sites [except O(3)]. Full-matrix unweighted least-squares refinement on  $I_o > 3 \sigma I$  gave  $R_{\text{obs}} = 2.6\%$  (1207 reflections) and  $R_{\text{all}} = 3.0\%$  (1355 reflections). Refined atom coordinates and displacement parameters, and selected bond lengths and angles are given in Tables 1 and 2, respectively. Observed structure factors have been deposited together with the crystallographic information file (deposited with the Principal Editor of *Mineralogical Magazine* and available from [http://www.minersoc.org/pages/e\\_journals/dep\\_mat\\_mm.html](http://www.minersoc.org/pages/e_journals/dep_mat_mm.html)).

The *a:b:c* ratio calculated from the unit-cell parameters is 0.540:1:0.297.

Powder X-ray diffraction data (CuK $\alpha$ ,  $\lambda = 1.54178 \text{ \AA}$ ) were obtained using the *XPREP* utility of *SAINTE* (Bruker, 2003), which generates a 2D powder diffractogram (Debye-Scherrer technique) starting from the  $F_o^2$  collected on the single crystal and taking into account solely the information concerning the unit-cell dimensions and the Laue symmetry. No Lorentz and polarization corrections were applied. Data are given in Table 3.

TABLE 1. Atom coordinates, refined site-scattering values\* (ss, epfu) and atom-displacement parameters ( $B_{eq}$ , Å<sup>2</sup>;  $\beta_{ij} \times 10^4$ ) for magnesio-riebeckite crystal 1303.

Site	ss	$x/a$	$y/b$	$z/c$	$B_{eq}$	$\beta^{11}$	$\beta^{22}$	$\beta^{33}$	$\beta^{12}$	$\beta^{13}$	$\beta^{23}$
O(1)		0.11125(14)	0.08913(8)	0.2104(3)	0.79(3)	22	6	83	-1	11	-2
O(2)		0.1180(2)	0.17052(8)	0.7357(3)	0.87(3)	26	6	93	0	10	-1
O(3)		0.1109(2)	0	0.7106(4)	0.94(5)	28	6	97	-	12	-
O(4)		0.3658(2)	0.25120(8)	0.7991(3)	1.08(3)	39	6	111	-4	18	1
O(5)		0.3520(2)	0.13162(8)	0.0861(3)	1.02(3)	28	9	89	0	12	8
O(6)		0.3428(2)	0.12116(8)	0.5800(3)	0.99(3)	29	9	80	0	11	-6
O(7)		0.3368(2)	0	0.2958(4)	1.14(5)	35	5	143	-	13	-
T(1)		0.28404(5)	0.08607(3)	0.29231(10)	0.69(2)	23	4	68	-1	11	-1
T(2)		0.29116(6)	0.17167(3)	0.80266(10)	0.72(2)	23	5	70	-1	12	0
M(1)	26.27(11)	0	0.08879(5)	1/2	0.78(2)	27	5	70	-	14	-
M(2)	43.24(13)	0	0.18091(3)	0	0.79(2)	26	5	78	-	13	-
M(3)	13.51(4)	0	0	0	0.75(3)	27	4	72	-	12	-
M(4)	23.6(2)	0	0.27537(7)	1/2	1.45(3)	47	11	148	-	47	-
A(m)	1.03(9)	0.033(3)	1/2	0.070(6)	2.0						
H	1.8(2)	0.198(7)	0	0.755(11)	1.0						

\*Hawthorne *et al.* (1995)**Chemical analysis**

Chemical analysis on the crystal used for structure refinement was done with a Cameca SX-100 electron microprobe (wavelength-dispersive spectroscopy

mode, 15 kV, 20 nA, counting time 20 s, beam diameter 5  $\mu$ m). The standards used are as follows: Si and Ca: diopside (TAP); Ti: titanite (LPET); Al: andalusite (TAP); Fe: fayalite (LLiF); Mn: spessartine (LLiF); Mg: forsterite (LTAP); Zn: gahnite (LLiF);

TABLE 2. Selected interatomic distances (Å), angles ( $^\circ$ ), bond angle variances ( $^\circ$ <sup>2</sup>) and quadratic elongations in magnesio-riebeckite crystal 1303.

T(1)-O(1)	1.622(2)	T(2)-O(2)	1.624(2)	M(4)-O(2) $\times$ 2	2.387(2)
T(1)-O(5)	1.621(2)	T(2)-O(4)	1.595(2)	M(4)-O(4) $\times$ 2	2.320(2)
T(1)-O(6)	1.623(2)	T(2)-O(5)	1.643(2)	M(4)-O(5) $\times$ 2	2.853(2)
T(1)-O(7)	<u>1.6191(8)</u>	T(2)-O(6)	<u>1.653(2)</u>	M(4)-O(6) $\times$ 2	<u>2.491(2)</u>
<T(1)-O>	1.621	<T(2)-O>	1.629	<M(4)-O>	2.513
TAV	1.19	TAV	15.41		
TQE	1.0003	TQE	1.0037		
M(1)-O(1) $\times$ 2	2.0703(14)	M(2)-O(1) $\times$ 2	2.1267(14)	M(3)-O(1) $\times$ 4	2.0903(14)
M(1)-O(2) $\times$ 2	2.079(2)	M(2)-O(2) $\times$ 2	2.0114(14)	M(3)-O(3) $\times$ 2	<u>2.067(2)</u>
M(1)-O(3) $\times$ 2	<u>2.0848(14)</u>	M(2)-O(4) $\times$ 2	<u>1.906(2)</u>	<M(3)-O>	2.082
<M(1)-O>	2.078	<M(2)-O>	2.015	OAV	58.13
OAV	47.99	OAV	38.62	OQE	1.0180
OQE	1.0144	OQE	1.0131		
O(5)-O(6)-O(5)	171.10(9)	T(1)-O(5)-T(2)	136.18(10)	A(m)-O(5) $\times$ 2	2.94(2)
O(6)-O(7)-O(6)	110.79(10)	T(1)-O(6)-T(2)	141.71(10)	A(m)-O(5) $\times$ 2	2.81(2)
		T(1)-O(7)-T(1)	143.7(2)	A(m)-O(6) $\times$ 2	2.92(2)
				A(m)-O(7)	2.47(3)
				A(m)-O(7)	3.30(3)
				A(m)-O(7)	<u>2.55(3)</u>
				<A(m)-O>	2.85

MAGNESIO-RIEBECKITE FROM THE VARENCHÉ MINE

TABLE 3. Powder X-ray data for magnesio-riebeckite, crystal 1303.

$I_{rel}$	$d(calc)$	$hkl$	$I_{rel}$	$d(calc)$	$hkl$	$I_{rel}$	$d(calc)$	$hkl$	$I_{rel}$	$d(calc)$	$hkl$
25.3	8.936	0 2 0	<b>62.2</b>	<b>3.079</b>	<b>3 1 0</b>	5.6	2.196	$\bar{2}$ 4 2	6.8	1.713	$\bar{5}$ 1 2
<b>82.7</b>	<b>8.303</b>	<b>1 1 0</b>	17.6	2.946	2 2 1	9.9	2.170	1 7 1	8.4	1.691	$\bar{1}$ 3 3
<b>29.7</b>	<b>4.855</b>	$\bar{1}$ 1 1	5.4	2.919	$\bar{1}$ 5 1	<b>30.0</b>	<b>2.155</b>	<b>2 6 1</b>	9.5	1.673	$\bar{2}$ 8 2
<b>49.9</b>	<b>4.467</b>	<b>0 4 0</b>	20.2	2.768	3 3 0	8.2	2.119	$\bar{3}$ 3 2	23.9	1.641	4 6 1
		<b>0 2 1</b>	<b>100.0</b>	<b>2.701</b>	<b>1 5 1</b>	13.9	2.062	2 0 2	9.6	1.617	4 8 0
5.3	4.152	2 2 0	<b>35.0</b>	<b>2.578</b>	<b>0 6 1</b>	13.5	2.010	3 5 1	12.2	1.601	1 11 0
10.4	3.850	$\bar{1}$ 3 1	<b>50.2</b>	<b>2.522</b>	$\bar{2}$ 0 2	9.1	1.981	4 0 2	21.3	1.582	$\bar{1}$ 5 3
8.9	3.623	$\bar{2}$ 2 1	<b>29.2</b>	<b>2.300</b>	$\bar{3}$ 5 1	5.1	1.871	2 4 2	7.8	1.561	6 0 0
<b>53.4</b>	<b>3.391</b>	<b>1 3 1</b>	20.6	2.277	$\bar{1}$ 7 1	5.9	1.865	5 1 0			4 0 2
8.7	3.342	1 5 0			$\bar{4}$ 2 1	9.3	1.848	$\bar{1}$ 9 1			
21.6	3.235	2 4 0	21.9	2.249	$\bar{3}$ 1 2	7.9	1.789	1 9 1			

Note: the strongest ten reflections are in bold. Only peaks with  $I_{rel} \geq 5$  are reported.

Na: albite (TAP); K: orthoclase (LPET); F: fluoro-riebeckite (TAP); Cl: tugtupite (LPET). H<sub>2</sub>O was estimated on the basis of 2=(OH,F,Cl) atoms per formula unit (apfu) and taking into account the constraints on the group-sites based on stoichiometry and site-scattering values (for A, B and C cations) obtained from the structure refinement; the same method allowed for Fe<sup>3+</sup>/Fe<sup>2+</sup> calculation. The oxide wt.% and the calculated unit formula are reported in Table 4. The proposed empirical formula for crystal 1303 is: <sup>A</sup>(Na<sub>0.09</sub>K<sub>0.01</sub>)<sub>Σ=0.10</sub> <sup>B</sup>(Na<sub>1.77</sub>Ca<sub>0.11</sub>Mg<sub>0.08</sub>Mn<sub>0.04</sub>)<sub>Σ=2.00</sub> <sup>C</sup>(Mg<sub>2.93</sub>Mn<sub>0.13</sub>Fe<sub>0.07</sub>Zn<sub>0.01</sub>Ni<sub>0.12</sub>Fe<sub>1.25</sub>Al<sub>0.48</sub>Ti<sub>0.01</sub>)<sub>Σ=5.00</sub> <sup>T</sup>(Si<sub>7.92</sub>Al<sub>0.08</sub>)<sub>Σ=8.00</sub>O<sub>22</sub> <sup>W</sup>(OH<sub>1.88</sub>F<sub>0.12</sub>)<sub>Σ=2.00</sub>.

**The crystal-chemistry of magnesio-riebeckite**

Site populations were obtained taking into account the experimental mean-bond lengths and site-scattering values for the individual sites (Oberti *et al.*, 2007). The results are reported in Table 5. <sup>T</sup>Al is ordered at the T(1) site and <sup>C</sup>R<sup>3+</sup> cations are ordered at the M(2) site. An even better agreement for the C-group cations could be achieved by allowing for some disorder of Ni (which has an ionic radius shorter than Mg and Fe<sup>2+</sup>, i.e. 0.69 Å vs. 0.72 and 0.78 Å, respectively; Shannon, 1976) between the M(1) and the M(2) sites.

We compare our results with the geometrical details of a riebeckite crystal with the crystal-

TABLE 4. Chemical composition (10 points), unit formula (based on 24 anions and 15.10 cations) and a comparison between observed and calculated site scattering for magnesio-riebeckite (1303).

Oxide	wt.%(esd)	Oxide	wt.%(esd)	apfu	apfu			
SiO <sub>2</sub>	57.10(27)	H <sub>2</sub> O*	1.80	Si	7.92	Na	1.77	
TiO <sub>2</sub>	0.09(1)	F	0.28(36)	Al	0.08	Ca	0.11	
Al <sub>2</sub> O <sub>3</sub>	3.41(5)	Cl	0.01(1)	Sum T	8.00	Mg	0.08	
Fe <sub>2</sub> O <sub>3</sub>	11.99	O = F,Cl	-0.12			Mn	0.04	
FeO	0.59	Total	100.08	Ti <sup>4+</sup>	0.01	Sum B	2.00	
[FeO] <sub>tot</sub>	[11.38(22)]			Al	0.48			
MgO	14.56(13)			Fe <sup>3+</sup>	1.25	Na	0.09	
MnO	1.40(9)	Group site-scattering (epfu)		Mg	2.93	K	0.01	
NiO	1.11(8)	obs (SREF)	calc (EMP)	Mn <sup>2+</sup>	0.13	Sum A	0.10	
ZnO	0.14(8)	C	83.02	82.87	Fe <sup>2+</sup>	0.07		
CaO	0.69(2)	B	23.58	23.57	Ni	0.12	(OH) <sup>-</sup>	1.88
Na <sub>2</sub> O	6.93(16)	A	1.03	1.21	Zn	0.01	F <sup>-</sup>	0.12
K <sub>2</sub> O	0.07(1)	Total	107.63	107.65	Sum C	5.00	Sum W	2.00

\* calculated based on 24 (O, OH, F, Cl) with (OH + F + Cl) = 2 apfu.

TABLE 5. Site populations for magnesio-riebeckite, crystal 1303. There is close agreement between the refined values of site-scattering (ss, electrons per formula unit) and mean bond-lengths (mbl, Å) and those calculated based on the proposed site-populations\*.

Site	Site population (apfu)	ss (epfu)		mbl (Å)	
		refined	calculated	refined	calculated
T(1)	3.89 Si+ 0.11 Al			1.621	1.622
T(2)	4.00 Si			1.629	
M(1)	1.89 Mg + 0.07 Fe <sup>2+</sup> + 0.04 Mn <sup>2+</sup>	26.27	25.50	2.078	2.080
M(2)	0.11 Mg + 0.13 Ni + 0.01 Zn + 1.25 Fe <sup>3+</sup> + 0.48 Al + 0.01 Cr + 0.01 Ti <sup>4+</sup>	43.24	44.46	2.015	2.008
M(3)	0.93 Mg + 0.07 Mn <sup>2+</sup>	13.51	12.91	2.082	2.083
Σ C cations		83.02	82.87		
B cations	1.74 Na + 0.10 Ca + 0.08 Mg + 0.04 Mn <sup>2+</sup>	23.58	23.57		
A cations	0.09 Na + 0.01 K	1.03	1.21		
W anions	1.88 (OH) <sup>-</sup> + 0.12 F <sup>-</sup>				

\*Hawthorne *et al.* (1995)

chemical formula  $A(K_{0.06}Na_{0.04})^B(Na_{1.86}Ca_{0.09}Fe_{0.05}^{2+})^C(Fe_{2.93}^{2+}Mg_{0.22}^{2+}Mn_{0.03}^{2+}Fe_{1.74}^{3+}Al_{0.07}^{3+}Ti_{0.01}^{4+})^T(Si_{7.95}Al_{0.05})O_{22}W(OH_{1.90}F_{0.10})$ . This crystal has been used to monitor, with single-crystal structure refinement, the high-temperature behaviour of riebeckite in Susta (2016) and Oberti *et al.* (2018), and was analysed after annealing according to the same EMPA procedures; it is hereafter defined as 1272 from its code in the CNR-IGG-Pv database. Coherently with the different Fe<sup>2+</sup> and Fe<sup>3+</sup> contents, the three independent octahedra have significantly different size and distortion in the two samples, as indicated by their values of octahedral angular variance (OAV) and octahedral quadratic elongation (OQE; Robinson *et al.*, 1971). Magnesio-riebeckite 1303 has: M(1): 2.078 Å, 47.99<sup>o</sup> and 1.0144; M(2): 2.015 Å, 38.62<sup>o</sup> and 1.0131; M(3): 2.082 Å, 58.13<sup>o</sup> and 1.0180. Riebeckite 1272 has: M(1): 2.114 Å, 51.61<sup>o</sup> and 1.0155; M(2): 2.027 Å, 39.63<sup>o</sup> and 1.0132; M(3): 2.119 Å, 72.11<sup>o</sup> and 1.0222). The sizes of the two independent tetrahedra are similar (magnesio-riebeckite 1303: <T(1)–O> = 1.621 Å, <T(2)–O> = 1.629 Å; riebeckite 1272: <T(1)–O> = 1.623 Å, <T(2)–O> = 1.629 Å). As a consequence, the chain of tetrahedra is somewhat more relaxed in magnesio-riebeckite 1303 than in riebeckite 1272 (O(5)–O(6)–O(5): 171.1° and O(6)–O(7)–O(6): 110.8° vs. 172.8° and 112.9°, respectively).

A further interesting feature of magnesio-riebeckite 1303, which is also observed in riebeckite 1272, is that the shape of the electron density at the

M(4) site is ellipsoidal with a larger β<sub>33</sub> component, but does not suggest cation ordering at different positions. Usually, a significant presence of small B cations that have a different local coordination more similar to the [6 + 2] coordination observed in <sup>B</sup>(Mg, Fe<sup>2+</sup>, Mn<sup>2+</sup>) amphibole, can be detected in the structure refinement *via* the need of a split M(4') position ~0.4 Å along the two-fold axis, which helps to model the electron density better.

In both compositions, the A cations are ordered at the A(m) position, which is shifted +/- 0.43 Å away from the centre of symmetry along the [1 0 2] lattice vector.

## References

- Baldelli, C., Dal Piaz, G.V. and Polino, R. (1983) Le quarziti a manganese e cromo di Varenche-St. Barthélemy, una sequenza di copertura oceanica della falda piemontese. *Ofioliti*, **8**, 207–221 [in Italian].
- Barresi, A.A., Kolitsch, U., Ciriotti, M.E., Ambrino, P., Bracco, R. and Bonacina, E. (2005) La miniera di manganese di Varenche (Aosta, Italia nord-occidentale): ardennite, arseniopleite, manganberzeliite, pirofanite, sarkinite, thortveitite, nuovo As-Sc-analogo della metavariscite e altre specie. *Micro*, **3**, 81–122 [in Italian].
- Bartelmehs, K.L., Bloss, F.D., Downs, R.T. and Birch, J. B. (1992) EXCALIBUR II. *Zeitschrift für Kristallographie*, **199**, 185–196.
- Bonazzi, P., Menchetti, S. and Reinecke, T. (1996) Solid solution between piemontite and androsite-(La), a new

- mineral of the epidote group from Andros Island, Greece. *American Mineralogist*, **81**, 735–742.
- Bruker (2003) *SAINT Software Reference Manual*. Version 6. Bruker AXS Inc., Madison, Wisconsin, USA.
- Castello, P. (1981) Inventario delle mineralizzazioni a magnetite, ferro-rame e manganese del complesso piemontese dei calcescisti con pietre verdi in Valle d'Aosta. *Oftoliti*, **6**, 5–46 [in Italian].
- Colville, A.A. and Gibbs, G.V. (1964) Refinement of the crystal structure of riebeckite. *Geological Society of America, Abstracts Annual Meetings*, **82**, 31.
- Dal Piaz, G.B., Di Battistini, G., Kienast, J.R. and Venturelli, G. (1979) Manganiferous quartzitic schists of the Piemonte ophiolite nappes in the Valsesia-Valtournanche area (Italian Western Alps). *Memorie di Scienze Geologiche*, **32**, 4–24.
- Ernst, W.G. (1957) *Annual Report, Geophysics Laboratory*. Carnegie Institute, Washington Year Book **56**, p. 228.
- Ernst, W.G. (1958) *Annual Report, Geophysics Laboratory*. Carnegie Institute, Washington Year Book **57**, p. 199.
- Ernst, W.G. (1959) *Annual Report, Geophysics Laboratory*. Carnegie Institute, Washington Year Book **58**, p. 121.
- Ernst, W.G. (1962) Synthesis, stability relations and occurrence of riebeckite and riebeckite-arfvedsonite solid solutions. *Journal of Geology*, **70**, 689–736.
- Ernst, W.G. (1968) *Amphiboles*. Springer-Verlag, New York, 125 pp.
- Hawthorne, F.C. (1978) The crystal structure and site chemistry of fluor-riebeckite. *Canadian Mineralogist*, **16**, 187–194.
- Hawthorne, F.C., Ungaretti, L. and Oberti, R. (1995) Site populations in minerals: terminology and presentation of results of crystal-structure refinement. *Canadian Mineralogist*, **33**, 907–911.
- Krause, L., Herbst-Irmer, R., Sheldrick, G.M. and Stalke, D. (2015) Comparison of silver and molybdenum microfocus X-ray sources for single-crystal structure determination. *Journal of Applied Crystallography*, **48**, 3–10.
- Le Bas, M.J., Le Maitre, R.W., Streckeisen, A. and Zanettin, B. (1986) A chemical classification of volcanic rocks based on the total alkali-silica diagram. *Journal of Petrology*, **27**, 745–750.
- Miyashiro, A. (1957) The chemistry, optics, and genesis of the alkali-amphiboles. *Journal of Faculty of Science, University of Tokyo, Section II*, **11**, 57–83.
- Miyashiro, A. and Iwasaki, M. (1957) Magnesioriebeckite in crystalline schists of Bizan in Sikoku, Japan. *Journal of the Geological Society of Japan*, **63**, 698–703.
- Robinson, K., Gibbs, G.V. and Ribbe, P.H. (1971) Quadratic elongation: a quantitative measure of distortion in coordination polyhedra. *Science*, **172**, 567–570.
- Oberti, R., Hawthorne, F.C., Cannillo, E. and Cámara, F. (2007) Long-range order in amphiboles. Pp. 125–172 in: *Amphiboles: Crystal Chemistry, Occurrence and Health Issues* (F.C. Hawthorne, R. Oberti, G. Della Ventura and A. Mottana, editors). Reviews in Mineralogy & Geochemistry, **67**. Mineralogical Society of America and the Geochemical Society, Chantilly, Virginia, USA.
- Oberti, R., Boiocchi, M., Zema, M., Hawthorne, F.C., Redhammer, G., Susta, U. and Della Ventura, G. (2018) The high-temperature behaviour of riebeckite: expansivity, deprotonation, selective Fe oxidation and a novel cation disordering scheme for amphiboles. *European Journal of Mineralogy*, in press.
- Sauer, A. (1888) Ueber Riebeckit, ein neues Glied der Hornblendegruppe, sowie über Neubildung von Albit in granitischen Orthoklasen. *Zeitschrift der Deutschen Geologischen Gesellschaft*, **40**, 138–152 [in German].
- Shannon, R.D. (1976) Revised effective ionic radii and systematic studies of interatomic distances in halides and chalcogenides. *Acta Crystallographica*, **A32**, 751–767.
- Sørensen, H. (editor) (1974) *The Alkaline Rocks*. John Wiley and Sons, London, 622 pp.
- Susta, U. (2016) *Dehydration and Deprotonation Processes in Minerals: Development of New Spectroscopic Techniques*. PhD Thesis, Università degli Studi Roma Tre, Italy, 177 pp.
- Whittaker, E.J.W. (1949) The structure of Bolivian crocidolite. *Acta Crystallographica*, **2**, 312–317.